This feasibility study suggests that this type of material has the potential to influence how implants are designed and could enable new surgical devices in the future.

References and Notes

1. J. G. Hunter, Ed., *Minimally Invasive Surgery* (McGraw-Hill, New York, 1993).
2. A. Charlesby, *Atomic Radiation and Polymers* (Pergamon, Oxford, 1960), pp. 198–257.
3. Y. Kagami, J. P. Gong, Y. Osada, *Macromol. Rapid Commun.* **17**, 539 (1996).
4. B. K. Kim, S. Y. Lee, M. Xu, *Polymer* **37**, 5781 (1996).
5. J. R. Lin, L. W. Chen, *J. Appl. Polym. Sci.* **69**, 1563 (1998).
6. ———, *J. Appl. Polym. Sci.* **69**, 1575 (1998).
7. T. Takahashi, N. Hayashi, S. Hayashi, *J. Appl. Polym. Sci.* **60**, 1061 (1996).
8. K. Sakurai, Y. Shirakawa, T. Kahiwagi, T. Takahashi, *Polymer* **35**, 4238 (1994).
9. K. Sakurai, T. Takahashi, *J. Appl. Polym. Sci.* **38**, 1191 (1989).
10. K. Sakurai, T. Kashiwagi, T. Takahashi, *J. Appl. Polym. Sci.* **47**, 937 (1993).
11. Y. Osada, A. Matsuda, *Nature* **376**, 219 (1995).
12. Z. Hu, X. Zhang, Y. Li, *Science* **269**, 525 (1995).
13. L. M. Schetky, *Sci. Am.* **241**, 68 (November 1979).
14. M. V. Swain, *Nature* **322**, 234 (1986).
15. A. Lendlein, A. Schmidt, R. Langer, *Proc. Natl. Acad. Sci. U.S.A.* **98**, 842 (2001).
16. A. Lendlein, P. Neuenschwander, U. W. Suter, *Macromol. Chem. Phys.* **201**, 1067 (2000).
17. H. G. Grablowitz, A. Lendlein, in preparation.
18. Both macrodiols were dissolved in 1,2-dichloroethane and heated to 80°C. An equimolar amount of 2,2(4),4-trimethylhexanediisocyanate was added. The synthesis was carried out under exclusion of water, and solvents and monomers were dried by standard techniques. The crude product was precipitated in hexane.
19. Data and video are available as supporting material on *Science* Online.
20. J. Van Humbeeck, *Mater. Sci. Eng.* **A273-275**, 134 (1999).
21. The material was pressed into films having a thickness of 300 to 500 μm. Dog bone–shaped samples (length between clamps, 6 mm; width, 3 mm) were punched out of the films and mounted in a tensile tester equipped with a thermo chamber (*8*, *21*). The tests were carried out at 200% strain at a strain rate of 10 mm min^{-1} with a low temperature (T_{low}) of –20°C and a high temperature (T_{high}) of 50°C. The samples were held at T_{low} for 10 min before the load was removed.
22. H. Tobushi, H. Hara, E. Yamada, S. Hayashi, *Soc. Photo-Opt. Instrum. Eng.* **2716**, 46 (1996).
23. H. Tobushi, S. Hayashi, A. Ikai, H. Hara, *J. Physique IV* **6**, C1-377 (1996).
24. A. F. T. Mak, M. Zhang, in *Handbook of Biomaterial Properties*, J. Black, G. Hastings, Eds. (Chapman and Hall, New York, ed. 1, 1998), pp. 66–69.
25. A. Lendlein, *Chem. Unserer Zeit* **33**, 279 (1999).
26. K. Fu, D. W. Pack, A. M. Klibanov, R. S. Langer, *Pharm. Res.* **17:1**, 100 (2000).
27. K. A. Hooper, N. D. Macon, J. Kohn, *J. Biomed. Mater. Res.* **32**, 443 (1998).
28. K. Spanel-Borowski, *Res. Exp. Med. (Berlin)* **189**, 69 (1989).
29. R. Crum, S. Szabo, J. Folkman, *Science* **230**, 1375 (1985).
30. J. Hoer, U. Klinge, A. Schachtrupp, Ch. Töns, V. Schumpelick, *Langenb. Arch. Surg.* **386**, 218 (2001).
31. N. C. F. Hodgson, R. A. Malthaner, T. Østbye, *Ann. Surg.* **231**, 436 (2000).
32. Control of stress was achieved on three levels: in the material itself through hard segment content, by programming, and during application through the looseness of the loops of the suture.
33. Extrusion was at 90°C through a 1-mm rod die on a Haake Polylab single-screw extruder.
34. Sterilization was done with ethylene oxide at 45°C.
35. The force of the fiber was determined with a tensile tester equipped with a thermo chamber. The force on the surrounding tissue was estimated by mounting a spring of known stiffness close to the wound and measuring the length change.
36. T_m and enthalpies ΔH_m of multiblockcopolymers were measured on a Perkin-Elmer DSC 7 at a heating rate of 10 K min^{-1}. The results were taken from the second heating run.
37. The weight content of ODX in the polymer is given by the two-digit number in the sample ID.

38. We thank H. Grablowitz for degradation experiments, J. Schulte for mechanical tests, W. Grasser for graphics, D. Rickert and M. Moses (Children's Hospital, Boston) for CAM tests, and R.-P. Franke (Zentralinstitut für biomedizinische Technik, University of Ulm) for the animal experiment. A.L. is grateful to Fonds der Chemischen Industrie for a Liebig fellowship. Partially funded by Bundesministerium für Bildung und Forschung BioFuture award no. 0311867.

Supporting Online Material
www.sciencemag.org/cgi/content/full/1066102/DC1
Tables S1 to S3
Movies S1 and S2

10 September 2001; accepted 11 April 2002
Published online 25 April 2002;
10.1126/science.1066102
Include this information when citing this paper.

Emerging Coherence in a Population of Chemical Oscillators

István Z. Kiss, Yumei Zhai, John L. Hudson*

Coherence of interacting oscillating entities has importance in biological, chemical, and physical systems. We report experiments on populations of chemical oscillators and verify a 25-year-old theory of Kuramoto that predicts that global coupling in a set of smooth limit-cycle oscillators with different frequencies produces a phase transition in which some of the elements synchronize. Both the critical point and the predicted dependence of order on coupling are seen in the experiments. We extend the studies both to relaxation and to chaotic oscillators and characterize the quantitative similarities and differences among the types of systems.

The collective behavior and synchronization of a population of somewhat dissimilar cyclic processes depend on the dynamics of the individual elements and on the interactions among them. Wiener raised the question of collective synchronization in a discussion of alpha rhythms in the brain (*1*). Synchronization has been shown to be an important process in the persistence of species (*2*) and in the functioning of heart pacemaker cells (*3*, *4*), yeast cells (*5*), and neurons in the cat visual cortex (*6*). Visual and acoustic interactions make fireflies flash (*7*), crickets chirp (*8*), and an audience clap in synchrony (*9*). Applications in engineering may be found in coupled chemical reactions (*10*, *11*), microwave systems (*12*), lasers (*13*), and digital-logic circuitry (*14*). Winfree (*4*) and Kuramoto (*15*, *16*) made a major advance in the theory of the onset of synchronization in populations with weak global coupling. In the model, each oscillator of an infinite set is described by a single variable, the phase, and is coupled to all other elements with equal strength. The theory predicts a transition with increasing global coupling strength (K) at which some of the oscillators with originally different frequencies become coherent, and it predicts the dependence of order on K above the critical point. The theory initiated extensive theoretical activity in collective dynamics and extensions to the effects of finite-size populations (*17*), fluctuations (*18*), and more complicated waveforms and coupling mechanisms (*19*, *20*). For a recent review, see (*21*). Simulations on arrays of Josephson junctions (*14*) and of lasers (*13*) have shown that coherent motion in physical systems can be interpreted using the Kuramoto model.

In this paper, we present results of a laboratory experiment that confirm the phase transition and dependence of order on coupling strength predicted by the theory on smooth limit-cycle oscillators (*16*). We show a strong enhancement of fluctuations near the critical point that arise in finite-size systems, in accordance with the theory of Daido (*17*). In addition, we extend the experiments to relaxation and chaotic (*22*) oscillators, which often occur in physical systems. We investigate the onset of coherence and the dependence of order and finite-size fluctuations on K, and we compare the characteristics of the three types of oscillators.

The experimental system is an array of 64 nickel electrodes in sulfuric acid (fig. S1). Current, which is proportional to the rate of metal dissolution, was measured on each electrode at a constant applied potential. Periodic or chaotic oscillations were observed, depending on conditions such as applied potential, acid concentration, and added external resistance (*23*, *24*). Inherent heterogeneities on the metal surface produced a distribution of frequencies of the oscillators. K was controlled through the use of

Department of Chemical Engineering, 102 Engineers' Way, University of Virginia, Charlottesville, VA 22904-4741, USA.

*To whom correspondence should be addressed. E-mail: hudson@virginia.edu

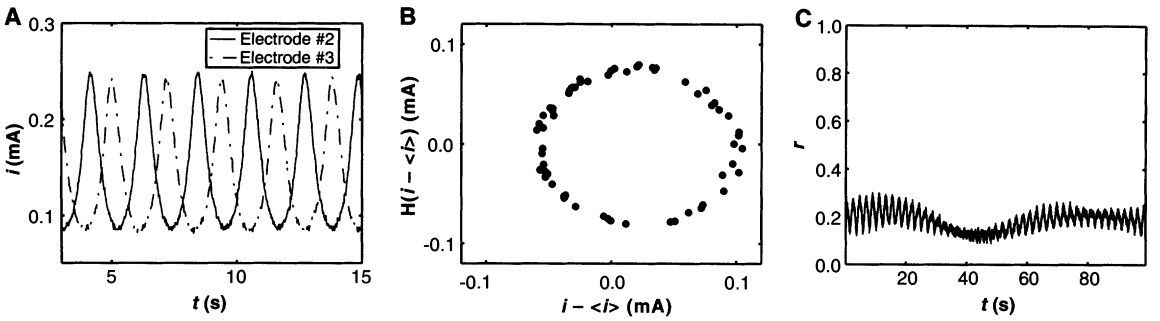

Fig. 1. The dynamics of 64 nonidentical periodic electrochemical oscillators without coupling. The currents of Ni electrodes (64 1-mm–in-diameter electrodes, in an 8 × 8 geometry, with 2-mm spacing) were measured at 100 Hz. The potential of each electrode was held at a constant potential (V) versus an Hg/Hg_2SO_4/concentrated K_2SO_4–reference electrode. A standard electrochemical cell was used with a Pt mesh counter electrode. The electrolyte was 3 M sulfuric acid at 11°C. The electrodes were connected to the potentiostat through one series (collective) resistor (R_s) and through parallel random resistors of mean R_p and a standard deviation of 21 ohms. Small random resistors were added to increase the variance of the frequency distribution; experiments without these resistors gave similar results to those shown, but with a slight loss in reproducibility. These random external resistors were not required in the experiments on chaotic oscillators. A global coupling parameter K is defined as $(R_s/R_{tot})/(1 - R_s/R_{tot})$, where R_{tot} is the total resistance ($R_{tot} = R_s + R_p/64$). (**A**) Current time series of two representative elements of the uncoupled array of periodic oscillators. $K = 0$, $V = 1.075$ V, $R_{tot} = 10.2$ ohms. (**B**) Phase portrait snapshot of the 64 oscillators. $\langle i \rangle$ is the temporal mean current, and H is the Hilbert transform. (**C**) Time series of order parameter $r(t) = |\Sigma_j \mathbf{P}_j(t)|/\Sigma_j |\mathbf{P}_j(t)|$, where $\mathbf{P}_j(t)$ are vectors of points in (B).

external series and parallel resistors; the total external resistance was held constant while the fraction dedicated to individual currents, as opposed to the total current, was varied.

Results obtained with periodic oscillators without added global coupling ($K = 0$) are shown in Fig. 1. As seen in two representative individual-current time series (Fig. 1A), the angular velocity is almost constant, although there is a slight slowing down at minimum values of the current. The natural frequency distribution is unimodal with the mean $\langle f \rangle = 0.4526$ Hz and the standard deviation $\sigma = 6.54$ mHz. We used the Hilbert transform H($i(t) - \langle i \rangle$), where H ($i(t) - \langle i \rangle$) =

$$1/\pi \int_{-\infty}^{\infty} (i(\tau) - \langle i \rangle)/(t - \tau) d\tau.$$

$i(t)$ is the current, and $\langle i \rangle$ is its temporal mean, to obtain the phase (*22*) of an individual oscillator. The points on a snapshot in H($i(t) - \langle i \rangle$) versus ($i(t) - \langle i \rangle$) space for the 64 oscillators are fairly well distributed on the limit cycle (Fig. 1B). The order parameter $r(t)$, defined as the normalized length of the vector sum of the phase points in Fig. 1B, is a measure of coherence; this parameter is similar to that introduced by Kuramoto in his study of coupled-phase oscillators (*18*). We confirmed that the specific definition of phase and order (*18*, 22) did not affect the results. The order parameter for the uncoupled set of 64 oscillators is shown in Fig. 1C. In the theory for an infinite set of oscillators, the parameter is constant and has a value of zero for $K < K_c$, where K_c is the critical point. The nonzero values obtained in the experiment can be attributed to the finite system size. A series of experiments with increasing number of oscillators ($N = 1, 2, 4, \ldots 64$) showed that the mean order parameter is proportional to $1/\sqrt{N}$.

The oscillator frequencies, as functions of their natural frequencies at three values of K, are shown in Fig. 2A. For K below K_c, deviations from the uncoupled case, the 45° line, are small. At K just above K_c (circles in Fig. 2A), the oscillators with frequencies near the mean become coherent, but those far above and far below the mean remain unsynchronized. This result is consistent with the original predictions of the theory (*18*). For larger values of K, additional oscillators become synchronized; for $K > 0.1$, all of the oscillators have the same frequency and fall on the horizontal line.

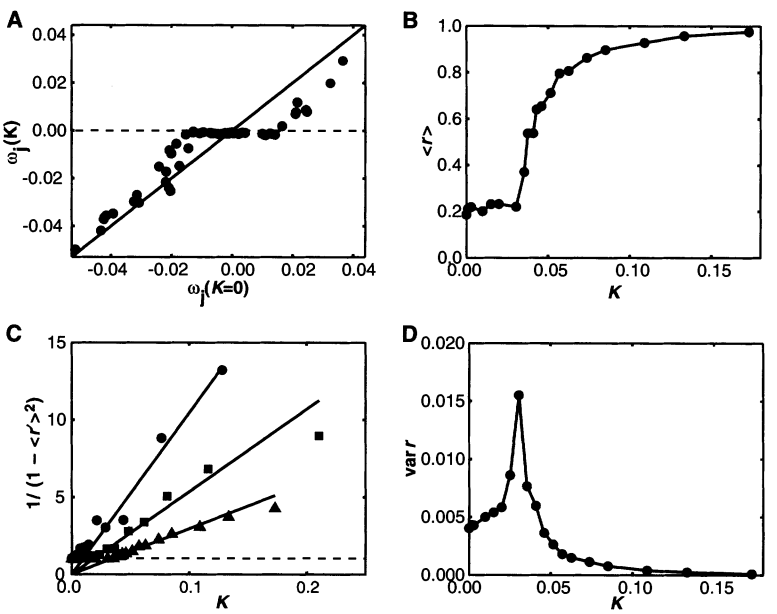

Fig. 2. The effect of global coupling on the coherence of periodic oscillators. (**A**) Dimensionless frequency $\omega_j = f_j/\langle f \rangle - 1$ (f_j is the frequency of the jth element, and $\langle f \rangle$ is the mean frequency) versus the corresponding frequencies without coupling ($K = 0$). Result obtained at $K = 0.034$, just above the critical coupling strength $K_c = 0.03$. The solid and dashed lines show the unsynchronized and completely synchronized cases, respectively. $V = 1.075$ V, $R_{tot} = 10.2$ ohms. (**B**) The mean order parameter $\langle r \rangle$ as a function of K. $V = 1.075$ V, $R_{tot} = 10.2$ ohms. (**C**) Linearized plot based on Kuramoto's theory. Dependence of order $1/(1 - \langle r' \rangle^2)$ on the coupling strength K at different experimental conditions. [$r' = (r - r_0)/(1 - r_0)$ was rescaled to 0 to 1 to remove the order at zero coupling (r_0) due to finite size.] The dashed line represents the following: $1/(1 - \langle r' \rangle^2) = 1$, i.e., $\langle r' \rangle = 0$. K_c is obtained from the slope of the fit ($1/K_c$). The circles represent the following: $K_c = 0.01$, $V = 1.090$ V, $R_{tot} = 7.1$ ohms. The squares represent the following: $K_c = 0.02$, $V = 1.085$ V, $R_{tot} = 8.6$ ohms. The triangles represent the following: $K_c = 0.03$, $V = 1.075$ V, $R_{tot} = 10.2$ ohms. (**D**) Variance of order parameter as a function of coupling strength. The curve was obtained by taking the mean of 10 experiments. The experimental conditions are the same as in (B).

The phase transition is quantitatively described with the mean order parameter $\langle r \rangle$ as a function of K (Fig. 2B). For small K, $\langle r \rangle \approx 0.2$, $\langle r \rangle$ was independent of K up to a critical value of 0.03. Above 0.03, $\langle r \rangle$ increased sharply with K. Kuramoto has shown analytically, for an infinite set of oscillators with a Lorentzian frequency distribution, that $r = \sqrt{1 - K_c/K}$ (*16*). The dependence of the or-

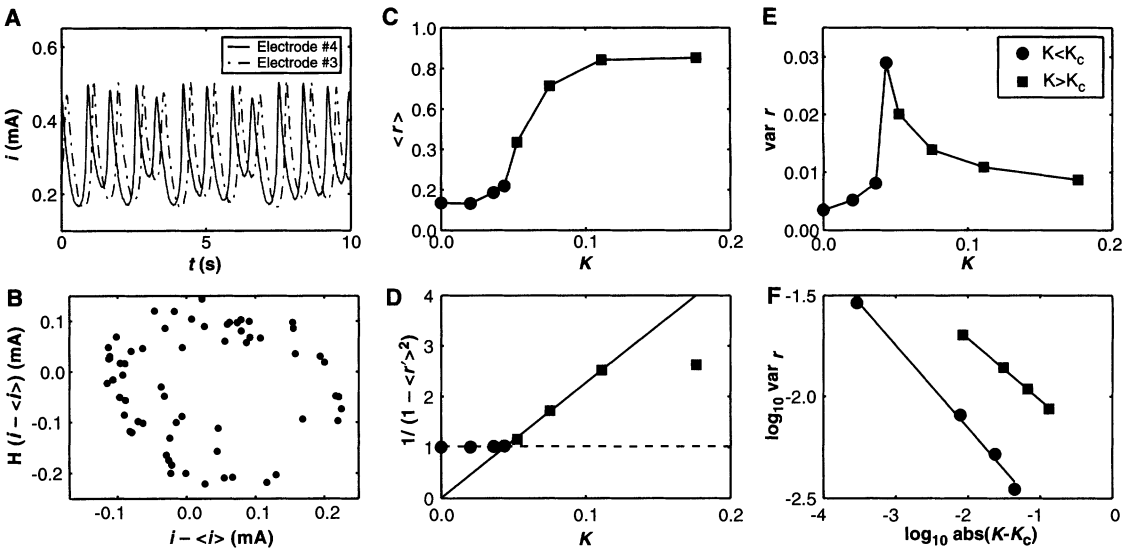

Fig. 3. The effect of global coupling on the coherence of chaotic oscillators. V = 1.310 V, R_{tot} = 14.2 ohms ($[H_2SO_4]$ = 4.5 M). **(A)** Time series of two representative elements. **(B)** Phase portrait snapshot of individual oscillators. **(C)** Mean order parameter as a function of coupling strength. **(D)** Linearized plot of order parameter as a function of coupling strength. The critical coupling strength is obtained from the slope of the line: 1/slope = K_c = 0.04. **(E)** Variance of the order parameter as a function of coupling strength. **(F)** Variance of order versus coupling strength on logarithmic plot. The slopes for $K < K_c$ and $K > K_c$ are −0.41 and −0.30, respectively.

der parameter (now r') on K is shown in Fig. 2C for three different conditions. r' has been rescaled from 0 to 1 to remove the order at zero coupling caused by the finite system size. All of the experiments are in accordance with the theoretical prediction. Below K_c, the quantity $1/(1 - r'^2)$ is 1, and above K_c it increases linearly with K with a slope of $1/K_c$.

The order parameter does vary with time in the experiments. The variance of r (Fig. 2D) has a maximum at K_c that is consistent with theoretical studies of systems of finite size (*17*). The order often undergoes large changes with time near $K = K_c$; for example, we have seen transitions from an almost unsynchronized behavior at $r = 0.3$ to an almost synchronized state at $r = 0.8$ in some experiments within a time frame of 20 oscillations.

We carried out the same type of experiments at a higher applied potential at which periodic relaxation oscillations are obtained; the frequency distribution ($\langle f \rangle$ = 0.35 Hz, σ = 39 mHz) is flatter and broader than that of the smooth oscillators considered above. There is again a critical coupling point at which the onset of synchronization is observed; K_c becomes larger as the circuit potential is increased, and the relaxation nature of the oscillations is more pronounced. The maximum in the variance of r (var r) at K_c is more than twice that seen in Fig. 2D. The transition from unsynchronized to coherent behavior occurs over a small range in coupling strength. Recent theoretical results on infinite-size systems predict a transition (depending on the nature of the relaxation oscillator) that is either less steep or discontinuous (*20*); the experimental results seem to be in agreement with the latter.

We also did such experiments with (weakly) chaotic oscillators (Fig. 3). The chaotic attractor is low dimensional and phase coherent. There is again a unimodal frequency distribution of the uncoupled 64 oscillators ($\langle f \rangle$ = 1.29 Hz, σ = 18 mHz); time series of two of the elements are shown in Fig. 3A. A snapshot of the uncoupled behavior in the H($i(t) - \langle i \rangle$) versus ($i(t) - \langle i \rangle$) space (Fig. 3B) shows that the points are distributed over the attractor. The effect of coupling is shown in the rest of Fig. 3. A phase transition occurs at K_c = 0.04 (Fig. 3C), and the dependence of r on K follows Kuramoto's theoretical prediction for $K < 0.15$ (Fig. 3D). However, the transition at K_c is not as sharp as it is in the periodic case; the somewhat gradual transition may be due to stronger effects of fluctuations (*22*). In addition, the order goes to 1 only at very large coupling strengths, where $K > 9$. There are deviations from the line in Fig. 3D for larger values of K, denoting less order than would be obtained with periodic oscillators. The same sharp maximum is seen for var r at K_c (Fig. 3E); var r scales as $|K - K_c|^{\alpha}$ with the scaling parameter (α) = −0.4 and −0.3 for $K < K_c$ and $K > K_c$, respectively (Fig. 3F). Daido showed in an analysis of large sets of phase oscillators (*17*) that α is −1 for $K < K_c$ and −¼ for $K > K_c$ but that the fit is very sensitive to finite-size effects, especially for $K < K_c$. Our results with 64 chaotic oscillators are consistent with the prediction for $K > K_c$. The periodic oscillators also followed a scaling law, although the exponents (α = −0.5 and −1.2 for $K < K_c$ and $K > K_c$, respectively) differ from the theoretical predictions; it may be that finite-size effects are stronger for periodic oscillators.

Thus, we see that results consistent with theory are obtained in laboratory experiments, even with a finite set of oscillators in the presence of unavoidable noise. At a critical coupling threshold, coherence emerges and some of the oscillators (with inherent frequencies near the mean) become synchronized. Above the critical value, the number of synchronized oscillators increases sharply. Finally, we see that the phase transitions and synchronization predicted in the theory are also obtained both for periodic relaxation oscillators and for coupled chaotic elements.

References and Notes

1. N. Wiener, *Nonlinear Problems in Random Theory* (MIT Press, Cambridge, MA, 1958).
2. B. Blasius, A. Huppert, L. Stone, *Nature* **399**, 354 (1999).
3. D. C. Michaels, E. P. Matyas, J. Jalife, *Circ. Res.* **61**, 704 (1987).
4. A. T. Winfree, *J. Theor. Biol.* **16**, 15 (1967).
5. A. K. Ghosh, B. Chance, E. K. Pye, *Arch. Biochem. Biophys.* **145**, 319 (1971).
6. C. M. Gray, P. Konig, A. K. Engel, W. Singer, *Nature* **338**, 334 (1989).
7. J. Buck, *Q. Rev. Biol.* **63**, 265 (1988).
8. T. J. Walker, *Science* **166**, 891 (1969).
9. Z. Néda, E. Ravasz, Y. Brechet, T. Vicsek, A. L. Barabási, *Nature* **403**, 849 (2000).
10. G. Ertl, *Science* **254**, 1750 (1991).
11. A. S. Mikhailov, A. Y. Loskutov, *Foundations of Synergetics II Chaos and Noise* (Springer, Berlin, 1996).
12. R. A. York, R. C. Compton, *IEEE Trans. Microw. Theory Tech.* **39**, 1000 (1991).
13. R. A. Oliva, S. H. Strogatz, *Int. J. Bifurcation Chaos* **11**, 2359 (2001).
14. K. Wiesenfeld, P. Colet, S. H. Strogatz, *Phys. Rev. Lett.* **76**, 404 (1996).
15. Y. Kuramoto, in *International Symposium on Mathematical Problems in Theoretical Physics, Lecture Notes in Physics*, H. Araki, Ed. (Springer, New York, 1975), vol. 39, pp. 420–422.
16. Y. Kuramoto, *Prog. Theor. Phys. Suppl.* **79**, 223 (1984).
17. H. Daido, *Prog. Theor. Phys.* **81**, 727 (1989).
18. Y. Kuramoto, *Chemical Oscillations, Waves and Turbulence* (Springer, Berlin, 1984).
19. R. E. Mirollo, S. H. Strogatz, *SIAM J. Appl. Math.* **50**, 1645 (1990).
20. H. Daido, *Phys. D* **91**, 24 (1996).
21. S. H. Strogatz, *Phys. D* **143**, 1 (2000).
22. A. S. Pikovsky, M. G. Rosenblum, G. V. Osipov, J. Kurths, *Phys. D* **104**, 219 (1997).
23. O. Lev, A. Wolffberg, M. Sheintuch, L. M. Pismen, *Chem. Eng. Sci.* **43**, 1339 (1988).
24. W. Wang, I. Z. Kiss, J. L. Hudson, *Phys. Rev. Lett.* **86**, 4954 (2001).

25. Supported by the NSF (CTS-0000483) and the Office of Naval Research (N00014-01-1-0603).

Supporting Online Material

www.sciencemag.org/cgi/content/full/296/5573/1676/DC1

Fig. S1

11 February 2002; accepted 3 April 2002